



Effects of TiO₂ and GO nanoparticles on the thermomechanical properties of bioactive poly-HEMA nanocomposites

Md. Alamgir¹ · G. C. Nayak² · Ashis Mallick¹ · Sumanta Sahoo²

Received: 7 October 2020 / Accepted: 1 June 2021 / Published online: 5 July 2021
© Iran Polymer and Petrochemical Institute 2021

Abstract

Bioactive polymeric nanocomposites are indispensable materials and have received great attention owing to their diverse applications in human body. In this study, a poly(hydroxyethyl methacrylate) (pHEMA) complex was prepared using hydroxyethyl methacrylate (HEMA) as a base material and trimethylolpropane trimethacrylate (TMPTA) and benzoyl peroxide (BPO) as cross-linking agents. The pHEMA nanocomposites were prepared by melt processing technique. In this process, a twin screw extruder machine was used. Twin screw extrusion is used extensively for mixing, compounding, or reacting polymeric materials. The flexibility of twin screw extrusion equipment allows this operation to be designed specifically for the formulation being processed. The nanocomposites of pHEMA/TiO₂ and pHEMA/TiO₂/GO were synthesized using pHEMA as a matrix with the addition of a small amounts of titanium oxide nanoparticles (TiO₂ 1 wt%) and graphene oxide (GO 0.1 wt%) as reinforcement materials. The thermomechanical study of pHEMA/TiO₂ and pHEMA/TiO₂/GO nanocomposites was carried out via thermogravimetric (TGA), differential scanning calorimetry (DSC), micro-indentation, micro-scratch, and FTIR analyses, and compression testing. The microstructural characterization of the nanocomposites was studied by FESEM and XRD analysis. Significant changes in microstructural behavior with improved thermomechanical properties were observed in pHEMA/TiO₂ and pHEMA/TiO₂/GO nanocomposites as compared to pure pHEMA. In this work, pure pHEMA and pHEMA/TiO₂ and pHEMA/TiO₂/GO nanocomposites were studied for dental applications.

Keywords pHEMA · Nanocomposites · Thermomechanical properties · Microstructure · Synthesis

Introduction

The selection of a polymer and its composite for dental application presents a great challenge for material scientists. The dental materials must have all biomimetic properties similar to those of the natural tooth tissues, i.e., being non-toxic, free from irritant ingredients, and insoluble in sputum. Thus, in the last few decades, substantial research efforts have been made toward the development of a new class of polymer nanocomposites that are suitable for dental applications.

Many approaches using polymeric nanocomposites have been attempted to develop novel materials for various

applications [1, 2]. Among them, the polymerization of hydrophilic monomers, such as 2-hydroxyethyl methacrylate (HEMA) and the synthesis of its nanocomposites are the most promising materials in biomedical applications [3, 4]. HEMA is one of the most common methacrylate monomers that are used as dental restitution materials [5, 6]. This material has a strong scaffolding property and can retain water; thus, has been deemed to be suitable for the use in biomedical devices. The polymerization process of HEMA depends on the combination of methacrylate groups and their structure. Owing to its excellent biocompatibility which mimics that of the living tissues, poly(hydroxyethyl methacrylate) (pHEMA) has been widely used for producing biomaterials such as dental epoxy resin and composite resin [7].

pHEMA has high permeability to small molecules and offers soft consistency that minimizes mechanical friction, resulting in the reduction of irritation to surrounding tissues [8, 9]. This polymer exhibits blood-compatibility and fine oxygen absorptivity. pHEMA is also resisted to thermal and chemical degradations [10, 11]. Pure pHEMA

✉ Ashis Mallick
mallick@iitism.ac.in

¹ Department of Mechanical Engineering, Indian Institute of Technology (ISM), Dhanbad 826004, Jharkhand, India

² Department of Chemistry, Indian Institute of Technology (ISM), Dhanbad, India

shows a glassy amorphous state with low water absorption and high adhesion to glass. This material has a low glass transition temperature (T_g) which depending on the conditions of the polymerization process varies between 50 °C and 90 °C [12].

A polymer composite as a dental material needs a significant volume fraction of inorganic reinforcement material in the cross-linked polymer matrix. Furthermore, to ensure the adhesion of matrix and reinforcement material, a coupling agent is required for their incorporation. Al-Jawoosh et al. [13] used propyl methacrylate as a coupling agent to support the chemical bonding between ceramic reinforcement material and polymer matrix.

The structural modification of a polymer by reinforcing it with nanoparticles has attracted a great attention in the last decade [14, 15]. A complete review of mesostructured polymeric nanocomposites was presented by Salimian et al. [16]. Biswas et al. [17] investigated the effect of aluminum particles reinforcement on the thermal and mechanical behavior of the unsaturated-polyester/jute nanocomposites. In their analysis, the micro-hardness values suggested that the nanocomposites were strengthened by the incorporation of 10 wt% reinforcement material, while 15 wt% reinforcement material exerted a negative effect (i.e., deterioration in strength) in the nanocomposites.

Thermal properties, such as thermal stability and residual mass were significantly enhanced with the addition of fillers. Ojha et al. [18] developed a carbon black reinforced polymer composite. Pyrolysis method at different carbonization temperatures was used to synthesize the natural carbon black particulates from an agriculture waste- wood-apple shell. They reported that the increase in the filler quantity and carbonization temperature improved the mechanical properties of the composites [18].

The composites and nanocomposites reinforced by conductive filler particles or fibers find plenty of use in electrical applications [19, 20]. Multi-walled carbon nanotubes (MWCNT) were incorporated in PVC (polyvinyl chloride) matrix using a roll mill technique for antistatic coating by Trommer et al. [21]. Polymeric nanocomposites (PNCs) exhibit superior properties as compared with straight micro- and macro-composites and can be obtained by joining nano-sized particles into polymeric matrices. PNCs have been widely investigated for many applications as they comprise the multifunctional properties of both organic and inorganic materials. PNCs are also known for their good mechanical, barrier, reduced solution uptake, and flammability properties [22]. The nanocomposite was described as an eco-friendly multifunctional material that can be reused for water remediation affecting photocatalytic characteristics. The physical, microstructural, mechanical, and expanding characteristics of the nanocomposites were examined to confirm the use of ZnO reinforcement over pure pHEMA material.

In the recent years, TiO₂ and GO nanoparticles have been extensively employed as active reinforcement materials in many metallic and polymeric matrix nanocomposites for improving the thermal and mechanical performance of the matrixes [23, 24]. The various strengthening mechanisms of matrixes in the presence of nano-reinforcements were discussed elsewhere [25]. Elashmawi et al. [26] synthesized and characterized PVDF/ PVC-based nanocomposites doped with graphene nanoparticles. In their study, they showed that GO nanoparticles stimulated the crystallin transformation in PVDF [26].

TiO₂ is known to be good multifunctional materials, having excellent mechanical properties and unique photo-induced activities. On the other hand, graphene-based nanoparticles have potential applications in the various fields of biomedical applications due to their antibacterial properties and tissue regenerative capacities [27]. The materials for dental applications, such as tooth structure, must tolerate a harsh oral environment and sustain occlusal loads arisen during biting, grinding and chewing.

Graphene oxide (GO) nanoparticles can easily be dispersed in water and organic solvents; which offers a distinct advantage in improving the various mechanical and physical properties of the polymer matrix. Graphene has very high electrical conductivity and can potentially be used in transport electrodes and nano-sensors [28]. Mosalman et al. [29] investigated the influence of TiO₂ nanoparticles as reinforcement on the mechanical properties of the polymethyl methacrylate (PMMA) nanocomposites prepared by injection molding. Prior to molding, the material was allowed to melt using a twin screw extruder. The results revealed an improvement in the flexural and impact strength of the composite due to the presence of TiO₂ nanoparticles [29]. Recently, Alamgir et al. [30] have presented a PMMA nanocomposite reinforced with TiO₂ and GO nanoparticles, together. In their study, mechanical and physical properties of the nanocomposite were determined and compared with those of the pure PMMA [30].

The main objective of the present work was to synthesize and characterize novel polymeric nanocomposites of pHEMA targeting for dental applications. The nanocomposites were synthesized by in-situ polymerization, followed by the melt processing utilization technique using a double screw extruder machine. The mechanical, thermal, and physical properties of the pHEMA nanocomposite have been explored. Poly(hydroxyethyl methacrylate) (pHEMA) was used as a base material for two different fillers, nano-TiO₂ powder, and GO nanoparticles. The sample materials were prepared at three different compositions. The first sample material was pure pHEMA, the second one contained pHEMA as matrix, and TiO₂ nanoparticles as reinforcement (pHEMA/TiO₂) in the weight ratio of 99:1 for pHEMA to TiO₂, and the third sample was pHEMA reinforced by TiO₂

and GO nanoparticles in the weight ratio of 98.9:1:0.1. The thermomechanical properties of the pHEMA nanocomposites were compared with those of the pure pHEMA. The nanocomposites showed improved hardness and elastic properties that seem to be suitable for dental applications.

Experimental

Materials

Pure graphite powder was used to produce graphene oxide (GO) using modified Hummers' method [31]. Other chemical reagents such as sulfuric acid (H_2SO_4 , 98%), potassium permanganate (KMnO_4), ortho-phosphoric acid (H_3PO_4 , 88%), selenium powder (particle size: 100 mesh), and hydrochloric acid (HCl, 10% concentrate) with a purity level of > 99.9% (supplied by Sigma Aldrich, India) were used to synthesize GO. The excess potassium permanganate (KMnO_4) was removed using hydrogen peroxide solution (H_2O_2 , 30% w/w), and then the GO solution was washed and dried for the use as filler material in the composite.

The monomer of 2-hydroxyethyl methacrylate (HEMA) with a purity level of > 98.5% was used as a matrix material. The cross-linking agent, trimethylolpropane trimethylacrylate (TMPTA) and benzoyl peroxide (BPO) with a purity level of > 98% were used for the polymerization of HEMA. The TiO_2 nanoparticles (with a purity level of about 99.9%) supplied by Alfa Aesar (USA) were also used as filler material in the nanocomposites. The molecular weight of the prepared polymers made them insoluble but, they could only be swelled in some solvents.

Preparation of GO nanoparticles

Improved Hummers' method was employed for the synthesis of graphene oxide. A sample of graphite nanoflakes (1 g) was added in a 30 mL mixture of sulfuric acid (98%) and orthophosphoric acid (88%) with a ratio of 3:1. The mixture was stirred at 5 °C temperature for 30 min, and then 5 g of KMnO_4 was added slowly to the above solution. After the addition of KMnO_4 , the mixture was further stirred at 50 °C for 24 h. To dilute the resulting graphite oxide nanoparticles, distilled water (600 mL) was added, and stirred at 500 RPM. The graphite oxide suspension was further treated with 30% H_2O_2 solution (5 mL) in a dark chamber for affirming the chemical reaction with KMnO_4 . To convert graphite oxide into graphene oxide, the resulting mixture was sonicated for 1 h, and then washed with HCl and H_2O followed by filtering in a filter paper. Further details pertaining to the production of pure GO nanoparticles is available elsewhere [30].

Polymerization

Poly(hydroxy ethyl methacrylate) (pHEMA) hydrogel samples were prepared by in situ polymerizations (0–70 °C for 2 h). In polymerization, hydroxyethyl methacrylate (HEMA) was used as a matrix material, and trimethylolpropane trimethacrylate and benzoyl peroxide (BPO) were used as polymerization initiators. The reagents were mixed in the following proportions: 50 mL of HEMA, 100 mL of trimethylolpropane trimethacrylate, and 1 g of benzoyl peroxide. After polymerization, about 150 g of pHEMA was obtained.

Preparation of pHEMA, pHEMA/ TiO_2 , and pHEMA/ TiO_2 /GO

The pHEMA nanocomposites were prepared by melt processing technique. In this process, a twin screw extruder machine was used. The pHEMA/ TiO_2 nanocomposite with TiO_2 nanoparticles as reinforcement was prepared in the weight ratio of 99:1 for pHEMA to TiO_2 , and the pHEMA/ TiO_2 /GO nanocomposite was prepared containing pHEMA reinforced by TiO_2 and GO nanoparticles in the weight ratio of 98.9:1:0.1.

The machine was operated at 270 °C with the shear rotation of 10 rpm for 10 min to ensure the proper homogeneous mixing as much as possible. The bulk samples of pure pHEMA and its nanocomposites were compression molded at 260 °C under a static pressure of 300 MPa for preparation of test samples for thermomechanical analysis and consequently, the samples were cooled to room temperature.

XRD analysis and ATR–FTIR spectroscopy

The crystallinity behavior of the pHEMA and its nanocomposites were examined by X-ray diffraction (XRD) analysis. Although attenuated total reflection-Fourier transform infrared (ATR-FTIR) spectroscopy analysis was performed to examine the chemical structure of compounds.

The XRD analyses were conducted using a Bruker (D8 Advance, Germany) X-ray diffractometer with reflection mode monochromatic Cu-K α radiation ($\lambda = 1.5408 \text{ \AA}$). The samples were scanned in 2θ , ranging from 20° to 60° with a scanning speed of 2° min^{-1} .

The FTIR spectral analysis was carried out by a Cary 630 (Agilent Technologies, USA) FTIR spectrometer operated in the ATR mode and contacting diamond ATR contact crystal. The spectra of the prepared pHEMA and its nanocomposites were recorded at room temperature in the region of 500–4000 cm^{-1} by 32 scans at a resolution of 4 cm^{-1} .

TGA

The specimens were investigated using thermogravimetric analysis (TGA) to determine the effect of filler content in the nanocomposites. The analyses were carried out by a thermal analyzer (SDT Q 600, TA instrument, USA) operated within a temperature range from 30 °C to 550 °C under a nitrogen environment. Each sample (20 mg) was heated at 10 °C/min. The weight loss with the increasing temperature was used to determine the thermal stability, degradation rate, and filler content.

DSC

Differential scanning calorimetry (DSC) analysis was performed by a thermal analyzer (SDT Q 600, TA instrument, USA) to determine the temperature associated with the various phase transitions and thermal performance of the materials. Each sample (20 mg) was heated from 30 °C to 450 °C at a heating rate of 10 °C/min in a nitrogen atmosphere. The endothermic and exothermic data of the samples were analyzed. The random inaccuracy of samples was identified for the selected composition.

Micro-indentation

The indentation module and Vickers hardness of the pHEMA and its nanocomposites were estimated using the micro-indentation test. Fully automated micro-indentation equipment (MTR3/50–50/NI, MICROTTEST SA, Spain) was used to perform the indentation test. The instrument was controlled by the Tribotester software associated with the instrument. The test was carried out under controlled force at the maximum indentation load of 5 N. The samples were unloaded after holding 30 s at 5 N loading.

Micro-scratch

Micro-scratch testing was performed using an acoustic emission based Microtest (MTR3/50–50/NI, Spain) scratch tester. A diamond tip indenter of radius 200 μm (indenter type Rockwell C) was employed for scratching the surfaces of the samples. A progressive load of 9.8 N was applied for initial penetration before starting the scratching. The samples were scratched for 6 mm in 1 min at a constant scratching speed. The scratching force and the coefficient were computed using the Tribotester software.

FESEM analysis

The fracture surface morphology and scratch surfaces of the bulk pHEMA and its nanocomposites were analyzed using a field emission scanning electron microscope (FESEM)

(Supra 55 Carl Zeiss, Germany). The fractured surfaces were obtained by breaking the samples in liquid nitrogen. The broken samples and the scratched samples were then coated with platinum to make sure the samples are conducting under an accelerating voltage of 5–15 kV.

Compression test

The compression tests for pHEMA and its nanocomposites were conducted at room temperature using a universal testing machine (H50KS, Hounsfield, UK). The cylindrical samples (as their both ends were completely flat) with 8 mm diameter and 8 mm length (ratio of length to diameter = 1) were molded in accordance with ASTM-E9-89a. During the test, the cylindrical samples were compressed gradually at a crosshead speed of 0.04 mm/min (i.e., strain rate = 8.3×10^{-5}). The samples of each composition were tested five times under the same testing condition, ensuring the consistency of the compressive behavior of the samples.

Results and discussion

Preparation of pHEMA, pHEMA/TiO₂, and pHEMA/TiO₂/GO

The formation of pHEMA is given schematically in Fig. 1. The pHEMA/TiO₂ nanocomposite was prepared by adding 1 wt% TiO₂ nanoparticles, while pHEMA/TiO₂/GO was prepared by adding 1 wt% TiO₂ nanoparticles and 0.1 wt% GO through polymerization. The addition of TiO₂ and GO nanoparticles had a large impact on the polymerization of pHEMA and its chemical and mechanical behavior. Figure 2 shows the schematic diagram of synthesis process of pHEMA/TiO₂, and pHEMA/TiO₂/GO nanocomposites.

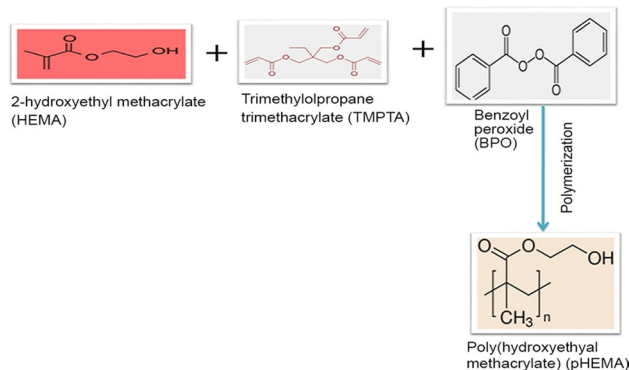


Fig. 1 Reaction route for polymerization of hydroxyethyl methacrylate (HEMA) to poly(hydroxyethyl methacrylate) (pHEMA)

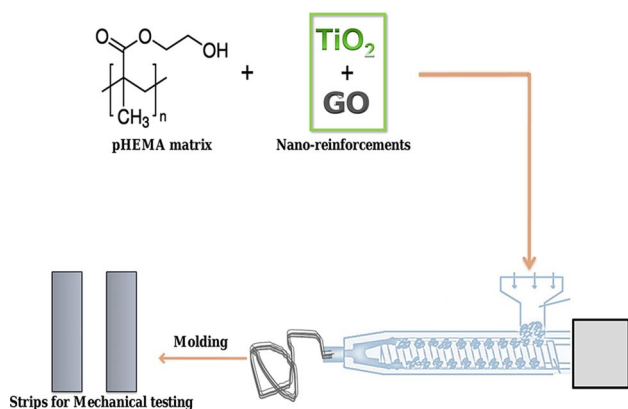


Fig. 2 Synthesis process of pHEMA/TiO₂ and pHEMA/TiO₂/GO nanocomposite samples

XRD and ATR-FTIR analyses

The XRD patterns and ATR-FTIR spectra of pure pHEMA and its nanocomposites are presented in Fig. 3a, b, respectively. As expected, the XRD profile of the pHEMA sample (Fig. 3a) did not reveal any sharp peaks indicating that an amorphous phase exists in pure pHEMA sample [32]. On the other hand, pHEMA/TiO₂ and pHEMA/TiO₂/GO patterns in Fig. 3a exhibited few sharp peaks indicating the formation of crystalline structure within the matrix of pHEMA. The sharp 2θ peaks near 23° to 25° in the nanocomposites confirmed the presence TiO₂ (mixed phase of TiO₂) nanoparticles in the pHEMA matrix. The sharp peak of GO was not visible in the XRD profile of the pHEMA/TiO₂/GO sample. This may be due to the small percentage of GO nanoparticles in the nanocomposite. However, the increase in the intensity and shifting of the TiO₂ peak could be ascribed to the presence of GO nanoparticles. Figure 3b represents the ATR-FTIR spectra of the pure pHEMA and its PNCs. The characteristic peaks of HEMA lies around 1715 cm⁻¹, 1630 cm⁻¹, and in the region 1361–1032 cm⁻¹ due to the C=O, C=C, and C–O–C stretching vibrations, respectively. In ATR-FTIR spectra of pHEMA, the peak corresponding to C=C, at 1630 cm⁻¹ was absent, and the peaks corresponding to C=O and C–O–C were present, which was the indicative of polymerization of the monomers and absence of side-chain cyclization [33]. A significant change in the peak positions and intensities in the spectra of pHEMA/TiO₂ and pHEMA/TiO₂/GO nanocomposites could be attributed to the appearance of new bands due to the presence of TiO₂ and GO nanoparticles. The ATR-FTIR spectra of pHEMA/TiO₂ and pHEMA/TiO₂/GO were characterized by the characteristic bands arising at 2924, 2852, and 1468 cm⁻¹ (Fig. 3b).

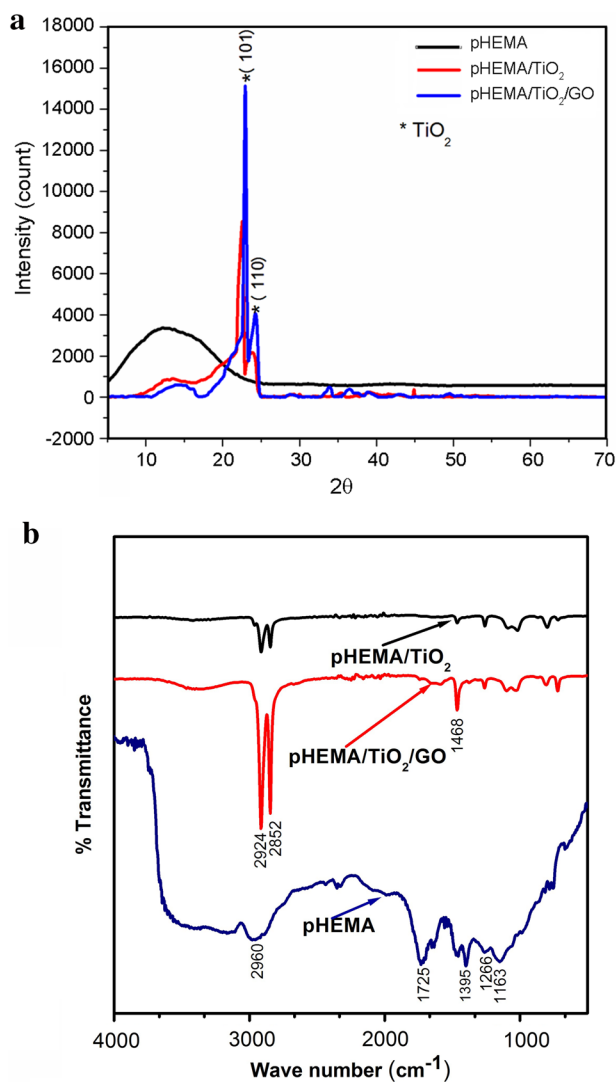


Fig. 3 a XRD patterns and b ATR-FTIR spectra of pure pHEMA, pHEMA/TiO₂, and pHEMA/TiO₂/GO samples

TGA analysis

The comparison of the residual weights of pHEMA and its nanocomposites as a function of temperature is presented in Fig. 4. The results clearly indicated that pHEMA and its nanocomposite are thermally stable up to a temperature of ~250 °C. A slight deviation in mass below 250 °C could be due to adsorbed moisture. A sharp weight loss was started at about 300 °C for all samples due to degradation of pHEMA [34]. It can be noticed that thermal degradation behavior of the nanocomposites was markedly different from that of pHEMA. At the temperature of 470 °C, the pHEMA sample was completely degraded, while decomposition of the nanocomposites occurred at higher temperature. This increase in the thermal stability could be ascribed to nanoparticles that induced restricted

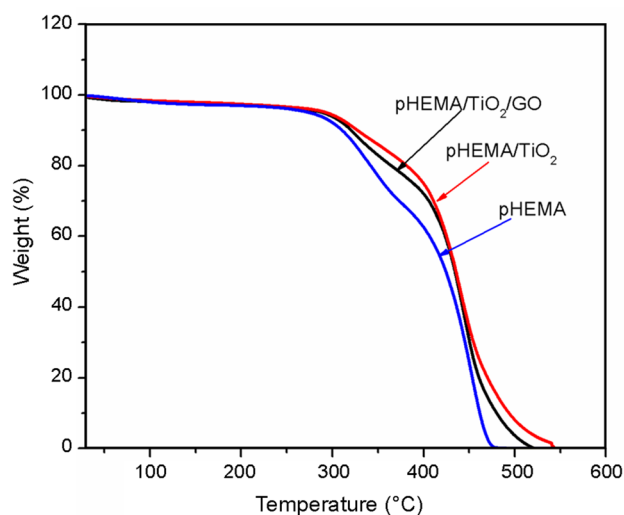


Fig. 4 TGA curves of pHEMA, pHEMA/TiO₂, and pHEMA/TiO₂/GO samples

thermal vibration at the particle polymer interfaces which required more energy for degradation when compared with virgin polymer.

In addition, nanoparticles, having high thermal conductivity, increase heat transfer rate that resulted in the uniform distribution of thermal energy within the nanocomposite, and hence delayed the degradation of the nanocomposites [35]. The interactions between the pHEMA matrix and nanoparticles also facilitated heat transfer from the matrix to nanoparticles, which are more thermally stable than the matrix. This transfer and distribution of thermal energy in the nanocomposites facilitated by nanoparticles increased the energy demand for their degradation, which resulted in better thermal stability of the nanocomposites in comparison to pHEMA. The pHEMA/TiO₂ nanocomposite containing 1 wt% TiO₂ nanoparticles revealed higher degradation temperature compared to pHEMA/TiO₂/GO nanocomposite reinforced with 1 wt% TiO₂ and 0.1 wt% GO nanoparticles. This result suggests that the former nanocomposite was more thermally stable than the latter one.

This observation can be explained on the basis of reduced polymeric chain interaction. Since GO nanoparticles contains many functional groups, they can better interact with polymer matrix which in turn can reduce the inter-polymeric cross-linking degree. In addition, GO nanoparticles have 2D nanostructures that can restrict polymer–polymer interactions which might be the reason for the reduced thermal stability of the pHEMA/TiO₂/GO nanocomposite. A similar trend was also reported for the nanoclay based epoxy nanocomposites where the 2D nano-sheets of nanoclay restricted cross-linking of the epoxy matrix and resulted in the reduction of thermal stability, as well [36].

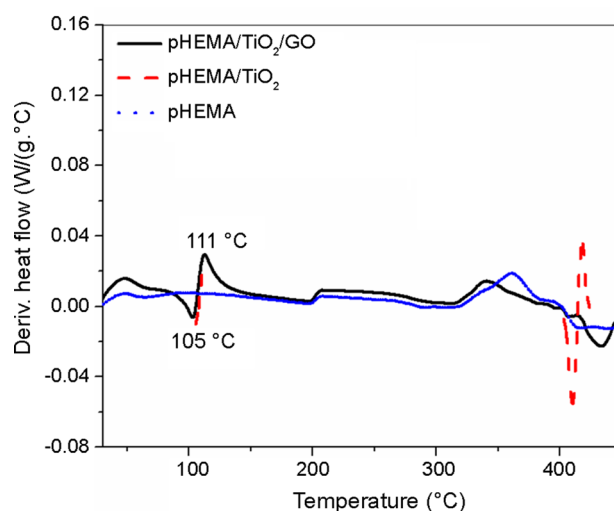


Fig. 5 DSC curves (exothermic up) showing glass transition (T_g) values of the prepared pHEMA, pHEMA/TiO₂, and pHEMA/TiO₂/GO samples

DSC analysis

The results of the DSC analyses are showed in Fig. 5 that revealed the various thermal transitions of pHEMA and its nanocomposites. The DSC measurements, performed on the dried sample of pHEMA, indicated glass transition temperature (T_g) of about 64 °C for pure pHEMA (Fig. 5). In contrast, the T_g for the nanocomposites was increased to 105 °C due to the presence of TiO₂ and GO nanoparticles. The enhancement in T_g of the composite samples was due to the presence of TiO₂ and GO nanoparticles that restricted the free movement of the polymer chain in the grafted-pHEMA. This attribute could be likely introduced by the cross-linking agent via the polymerization of the growing pHEMA/TiO₂ or pHEMA/TiO₂/GO polymeric chains. The endothermic peaks at 410 °C and 435 °C observed in the DSC curves of pHEMA/TiO₂ and pHEMA/TiO₂/GO nanocomposites, correspondingly, can be ascribed to the degradation of pHEMA matrix.

Micro-hardness analysis

The micro-indentation tests were performed to measure the hardness of pHEMA and its nanocomposites, i.e., pHEMA/TiO₂ and pHEMA/TiO₂/GO samples. An indentation force of 5 N was applied for all the samples through Vickers micro indenter, corresponding to different penetration depth for different samples, as expected. The representative curves of load–penetration ($P-h$) for pHEMA and its nanocomposites are presented in Fig. 6. The penetration depth was observed to be the maximum value for pHEMA sample, followed by pHEMA/TiO₂/GO and pHEMA/TiO₂ samples. The ability to

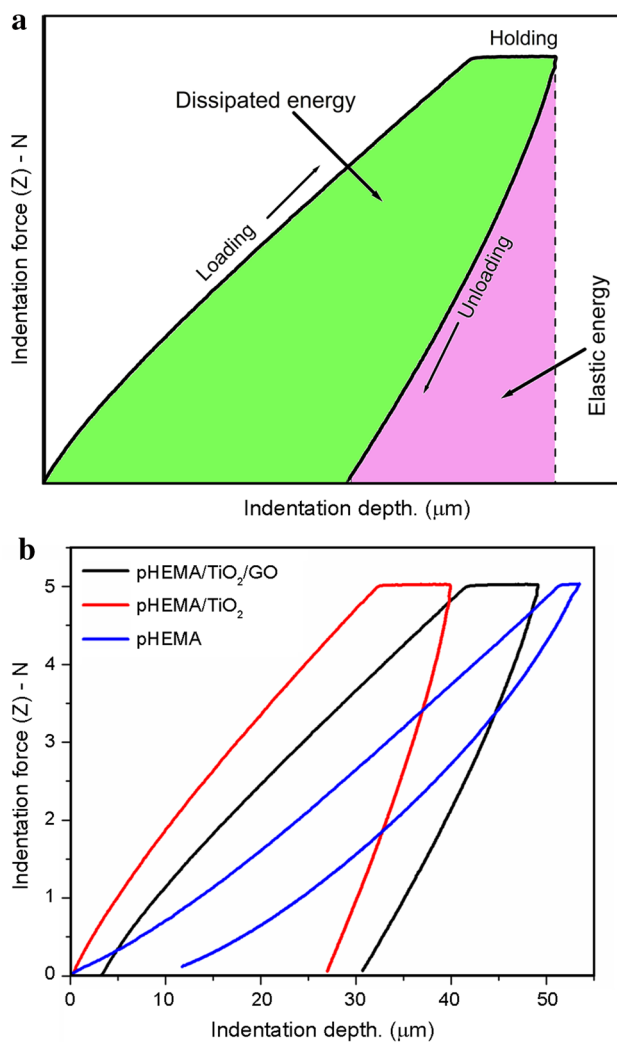


Fig. 6 **a** A typical loading–unloading curve, **b** variation of loading–unloading curves of pHEMA, pHEMA/TiO₂, and pHEMA/TiO₂/GO samples for micro-indentation test

retain elastic energy of each sample was estimated from the loading–unloading curves. The higher slopes for loading and unloading curves were observed for pHEMA/TiO₂ samples, followed by pHEMA/TiO₂/GO and pHEMA samples.

The results of micro-hardness, maximum penetration depth, indentation modulus, dissipated energy and retain

elastic relaxation are presented in Table 1. It can be seen that the incorporation of a small amount of TiO₂ nanoparticles (1 wt%) significantly improved the hardness and indentation modulus of nanocomposite as compared to pure pHEMA.

The plastic deformation in pure pHEMA mainly occurs by the nucleation and unhindered movements of shear bands. In contrast, the improvement in the presence of TiO₂ nanoparticles can be ascribed to the annihilation of vacancy cluster and free volume in the nanocomposite. TiO₂ nanoparticles offered good mechanical interlocking that acted against the propagation of shear bands. On the other hand, the presence of GO nanoparticles (0.1 wt%) in the pHEMA/TiO₂/GO nanocomposite diminished the values of micro-hardness and indentation modulus as compared to those of the pHEMA/TiO₂ nanocomposite. The factor that mitigated further improvement in the micro-hardness and indentation modulus could be the poor dispersion of GO nanoparticles in the pHEMA/TiO₂/GO nanocomposite. In fact, the agglomeration of GO nanoparticles and a large number of micropores negatively affected the micro-hardness value of its nanocomposite sample. Li et al. [37] reported similar findings regarding the flexural and compressive strengths after the incorporation of GO.

The ratio of retain elastic energy to the total indentation work (U_E/U_T) was estimated 0.666 for pure pHEMA, suggested sink-in dominated deformation mechanism. Deformation mechanism refers to the various processes occurring at micro-scale that are responsible for changes in a material's internal structure, shape, and volume. On the other hand, a lower ratio of retaining elastic energy to the total indentation work suggest that possibly pile-up mechanism could be associated in the deformation of the nanocomposites [38].

Micro-scratch analysis

The response of sliding contact in terms of abrasion was monitored. An indentation force of 9.8 N was applied in order to obtain the initial penetration (about 50.4 μm deep) before beginning the process of scratching. The scratch groves were examined by FESEM to ascertain the adhesion behavior of the fillers particles in the nanocomposites (Fig. 7). When comparing the scratch groves on the surface of pHEMA/TiO₂ nanocomposite (Fig. 7a) with

Table 1 Comparison of maximum penetration depth, indentation module, Vickers hardness, dissipated energy and elastic energy of pHEMA, pHEMA/TiO₂, and pHEMA/TiO₂/GO samples

Sample code	Indentation test ($P_{max} = 5$ N, holding time = 30 s)					
	Penetration depth (μm)	Indentation module (GPa)	Vickers hardness (kg/mm ²)	Elastic energy (U_E) (μJ)	Dissipated energy (U_p) (μJ)	U_E/U_T
pHEMA	53.52	1.0	14.3 ± 0.6	84.87	42.52	0.665
pHEMA/TiO ₂	39.95	3.2	17.3 ± 0.68	28.15	97.70	0.224
pHEMA/TiO ₂ /GO	49.16	1.9	15.2 ± 0.57	40.54	99.98	0.288

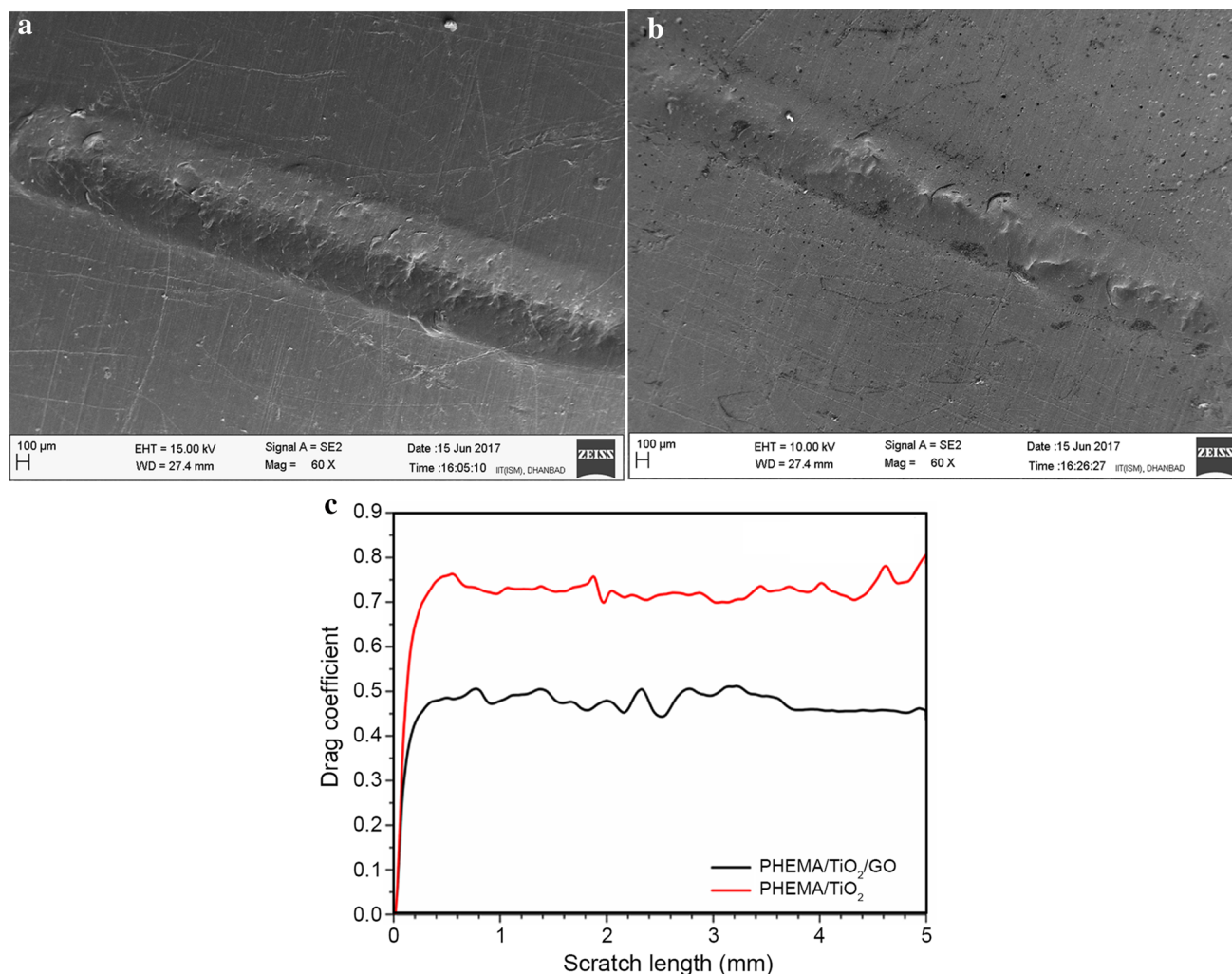


Fig. 7 FESEM micrographs of the surface topography of the scratched surfaces: **a** pHEMA/TiO₂ and **b** pHEMA/TiO₂/GO; **c** variation of drag coefficient of pHEMA/TiO₂ and pHEMA/TiO₂/GO samples along the scratch length

the comparatively smooth scratch tracks on the surface of pHEMA/TiO₂/GO nanocomposite (Fig. 7b) confirmed that GO nanoparticles acted as a solid lubricant.

The representative plots of the variations in the drag coefficient along the scar length are presented in Fig. 7c. Minor variations in the drag coefficients along the scar were observed in both the samples. A reasonably lower drag coefficient (about 30–40%) was observed for the pHEMA/TiO₂/GO nanocomposite than the pHEMA/TiO₂ sample. This result further indicated that presence of GO nanoparticles reduced the frictional force in the pHEMA/TiO₂/GO nanocomposite, in accordance with the effect of internal lubrication. In contrast, absence of the effective solid lubrication resulted in a rough scar surface with multiple micro-contact damaged features on the pHEMA/TiO₂ nanocomposite surface.

FESEM analysis

The surface morphologies of the fractured samples of pHEMA, pHEMA/TiO₂, and pHEMA/TiO₂/GO examined by FESEM technique are presented in Fig. 8. The FESEM micrograph of pure pHEMA showed smooth morphology which was corresponded to its brittleness (Fig. 8a).

However, in the presence of TiO₂ nanoparticles (Fig. 8b), the surface became bumpy, an indication of better interfacial adhesion and restricted crack propagation. Thus, the hard filler material like TiO₂ nanoparticles offered high toughness in the nanocomposite which can be used as a promising denture base material with high integrity in mechanical properties.

Further addition of GO nanoparticles led to slightly flat surfaces, which is an indication of better lubrication

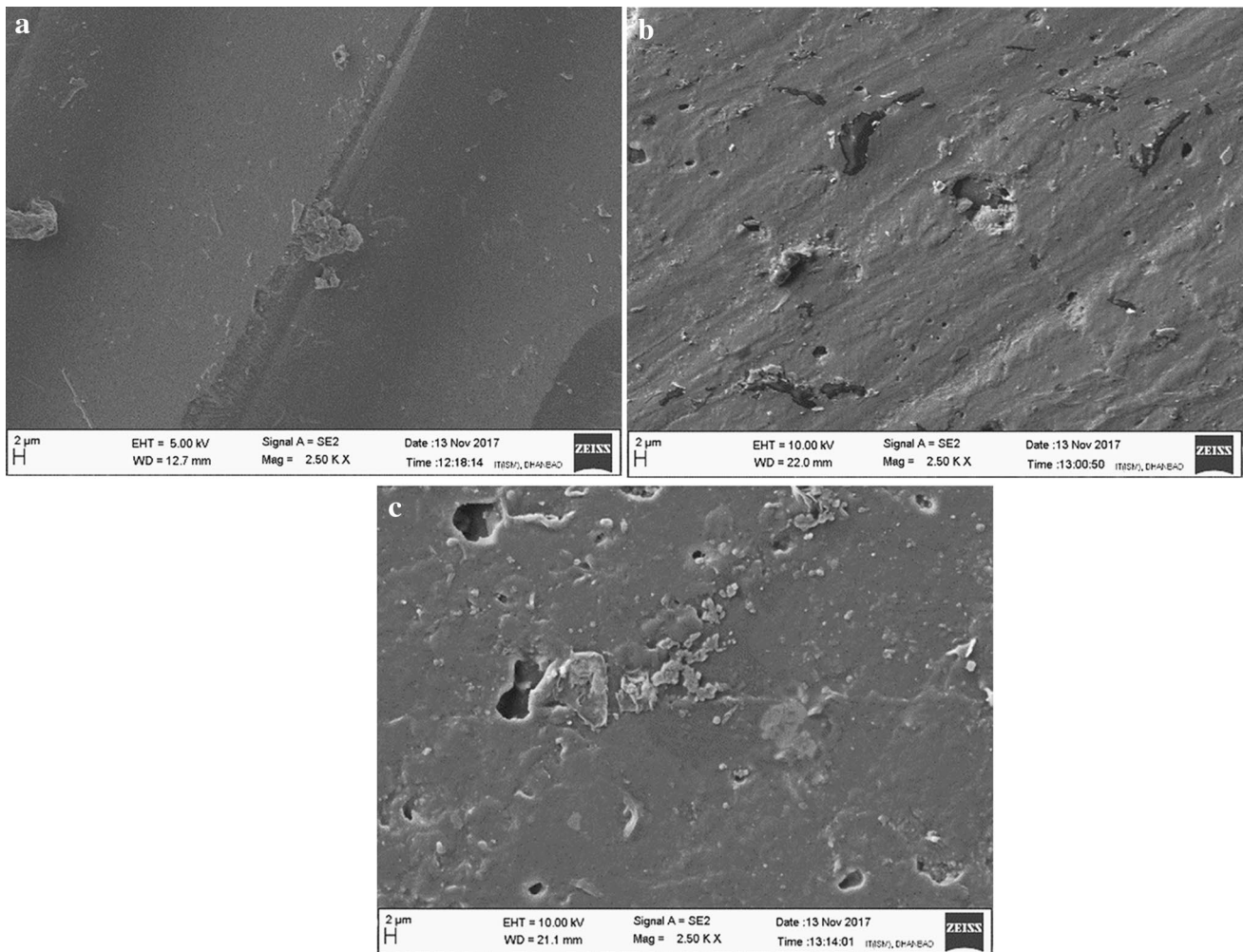


Fig. 8 FESEM micrographs of **a** pure pHEMA, **b** pHEMA/TiO₂ and **c** pHEMA/TiO₂/GO samples

properties under scratch (Fig. 8c). In addition to the roughness, some holes were also observed in the fractured surface, which could be due to agglomerated nanoparticles that might have been pulled out during the fracture.

Compression analysis

The typical load–displacement curves of pHEMA/TiO₂ and pHEMA/TiO₂/GO nanocomposites obtained by means of compression tests are given in Fig. 9. Both samples were deformed in a rubbery manner and a post-yield softening behavior was observed. Although, the apparent post-yield softening in pHEMA/TiO₂/GO nanocomposite was more pronounced than that in pHEMA/TiO₂ sample. The increase in the compressive load with the displacement after post-yield softening was observed in pHEMA/TiO₂ sample. This could be a result of densification of the sample. On the other hand, a significant reduction in the strength of the pHEMA/TiO₂/GO sample was observed compared to that of the

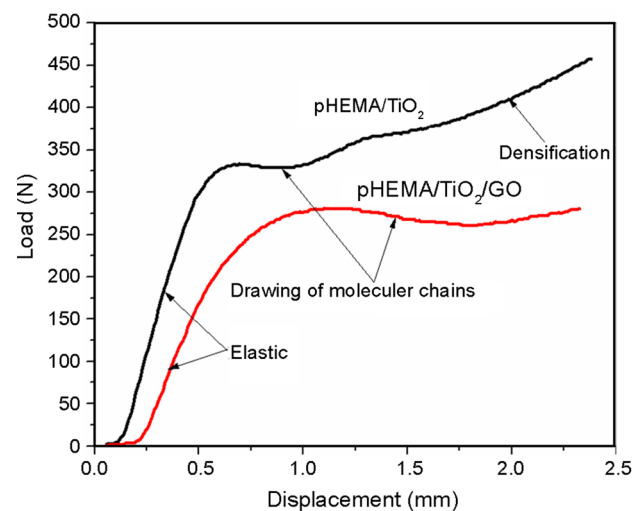


Fig. 9 Load–displacement curves of pHEMA/TiO₂ and pHEMA/TiO₂/GO nanocomposites

pHEMA/TiO₂ sample. The elastic modulus (E) of the nanocomposites was estimated from the tangent of the load–displacement curve in the elastic region under compression. Elastic modulus is mainly affected by the volume and stiffness of a nanocomposite. The density (ρ) of each sample was measured using Archimedes' principle. The specific stiffness (E/ρ) values of ~69.15 and 53.49 were found for pHEMA/TiO₂ and pHEMA/TiO₂/GO nanocomposites, respectively. The specific strengths (σ/ρ) of ~3.06 and 2.47 kN.m/kg were estimated for pHEMA/TiO₂ and pHEMA/TiO₂/GO nanocomposites, respectively. The reduction in specific strength and stiffness of the pHEMA/TiO₂/GO nanocomposite may be due to the elongated drawing of the molecular chains in the presence of GO nanoparticles.

Conclusion

In this study, nanocomposites of poly(hydroxyethyl methacrylate) (pHEMA) reinforced with 1 wt% TiO₂ nanoparticles and/or 0.1 wt% of graphene oxide (GO) nanoparticles were synthesized by using a twin screw extruder. X-ray and FTIR analyses revealed that a small amount of TiO₂ and GO nanoparticles promoted the crystal transformation of the nanocomposites. The TGA and DSC analyses revealed that the thermal stability of the nanocomposites was much better than that of the pure pHEMA. A significant improvement in mechanical properties, such as micro-hardness, compressive strength, and elastic modulus was observed due to the presence of TiO₂ nanoparticles in pHEMA/TiO₂ nanocomposite. In contrast, these mechanical properties were slightly degraded when GO nanoparticles were added as reinforcement. A lower drag coefficient was observed for pHEMA/TiO₂/GO nanocomposite on account of the presence of GO nanoparticles, which offered better lubrication properties.

Acknowledgements This research work was funded and supported by SERB, Department of Science and Technology, Govt. of India, under a research Grant (No. DST/SB/EMEQ/020/2013).

References

- Nelson JK (2010) Dielectric nanocomposite polymers. Springer, New York
- Koo JH (2006) Polymer nanocomposites: processing, characterization, and applications. McGraw-Hill, New York
- Montheard J-P, Chatzopoulos M, Chappard D (1992) 2-Hydroxyethyl methacrylate (HEMA): chemical properties and applications in biomedical fields. *J Macromol Sci Polym Rev* 32:1–34
- Achilias DS, Siafaka PI (2017) Polymerization kinetics of poly(2-hydroxyethyl methacrylate) hydrogels and nanocomposite materials. *Processes* 5:21. <https://doi.org/10.3390/pr5020021>
- Kopperud HM, Kleven IS, Wellendorf H (2011) Identification and quantification of leachable substances from polymer-based orthodontic base-plate materials. *Eur J Orthod* 33:26–31
- Park J-G, Ye Q, Topp EM, Kostoryz EL, Wang Y, Kieweg SL, Spencer P (2008) Preparation and properties of novel dentin adhesives with esterase resistance. *J Appl Polym Sci* 107:3588–3597
- Yourtee DM, Smith RE, Russo KA, Burmaster S, Cannon JM, Eick JD, Kostoryz EL (2001) The stability of methacrylate biomaterials when enzyme challenged: kinetic and systematic evaluations. *J Biomed Mater Res* 57:522–531
- Schweikl H, Spagnuolo G, Schmalz G (2006) Genetic and cellular toxicology of dental resin monomers. *J Dent Res* 85:870–877
- Jung Y-J, Hyun H-K, Kim Y-J, Jang K-T (2009) Effect of collagenase and esterase on resin-dentin interface: a comparative study between a total-etch adhesive and a self-etch adhesive. *Am J Dent* 22:295–298
- Rayment EA, Dargaville TR, Shooter GK, George GA, Upton Z (2008) Attenuation of protease activity in chronic wound fluid with bisphosphonate-functionalized hydrogels. *Biomaterials* 29:1785–1795
- Schiraldi C, Agostino AD, Oliva A, Flamma F, De Rosa A, Apicella A, Aversa R, De Rosa M (2004) Development of hybrid materials based on hydroxyethylmethacrylate as supports for improving cell adhesion and proliferation. *Biomater* 25:3645–3653
- Bolbukh Y, Klonos P, Roumpos K, Chatzidogiannaki V, Tertykh V, Pissis P (2016) Glass transition and hydration properties of polyhydroxyethylmethacrylate filled with modified silica nanoparticles. *J Therm Anal Calorim* 25:1387–1398
- Al-Jawoosh S, Ireland A, Su B (2018) Fabrication and characterisation of a novel biomimetic anisotropic ceramic/polymer-infiltrated composite material. *Dent Mater* 34:994–1002
- Pyrzynski K, Nyszko G, Zaikov GE (2015) Chemical and structure modification of polymers. Apple Academic Press, New York
- Madhumitha G, Fowsiya J, Roopan SM, Thakur VK (2018) Recent advances in starch–clay nanocomposites. *Int J Polym Anal Char* 23:331–345
- Salimian S, Zadhoush A, Mohammadi A (2018) A review on new mesostructured composite materials: part I. synthesis of polymer-mesoporous silica nanocomposite. *J Reinf Plast Compos* 37:441–459
- Biswas B, Chabri S, Sawai P, Mitra BC, Das K, Sinha A (2018) Effect of aluminum addition on the mechanical and thermal behavior of unsaturated polyester/jute composites. *Adv Polym Technol* 37:810–821
- Ojha S, Acharya SK, Raghavendra G (2015) Mechanical properties of natural carbon black reinforced polymer composites. *J Appl Polym Sci* 132:41211. <https://doi.org/10.1002/app.41211>
- Hussien B, Hashim A, Jewad A (2012) Electrical properties of polyvinylchloride-Zinc composite. *Eur J Soc Sci* 32:225–229
- Fu X, Al-Jumaily AM, Ramos M, Chen Y-F (2018) Comprehensive analysis on the electrical behavior of highly stretchable carbon nanotubes/polymer composite through numerical simulation. *J Mater Res* 33:3398–3407
- Trommer K, Petzold C, Morgenstern B (2014) Processing and properties of carbon nanotube PVC composites. *J Appl Chem*. <https://doi.org/10.1155/2014/307274>
- Selvi J, Parthasarathy V, Mahalakshmi S, Anbarasan R, Daramolala MO, Kumar PS (2020) Optical, electrical, mechanical, and thermal properties and non-isothermal decomposition behavior of poly(vinyl alcohol)–ZnO nanocomposites. *Iran Polym J* 29:411–422
- Polizos G, Tuncer E, Sauers I, James DR, Ellis AR, More KL (2010) Electrical and mechanical properties of titanium dioxide nanoparticle filled epoxy resin composites. *AIP Conf Proc* 1219:41–46
- Bayani M, Ehsani M, Khonakdar HA, Seyfi J, HosseinAbadi-Ghaeni MH (2017) An investigation of TiO₂ nanoparticles effect

- on morphology, thermal, and mechanical properties of epoxy/silica composites. *J Vinyl Addit Technol* 23:E216–E221
25. Casati R, Vedani M (2014) Metal matrix composites reinforced by nano-particles—a review. *Metals* 4:65–83
 26. Elashmawi IS, Alatawi NS, Elsayed NH (2017) Preparation and characterization of polymer nanocomposites based on PVDF/PVC doped with graphene nanoparticles. *Res Phys* 7:636–640
 27. Ge Z, Yang L, Xiao F, Wu Y, Yu T, Chen J, Lin J, Zhang Y (2018) Graphene family nanomaterials: properties and potential applications in dentistry. *Int J Biomater*. <https://doi.org/10.1155/2018/1539678>
 28. Gómez-Navarro C, Weitz RT, Bittner AM, Scolari M, Mews A, Burghard M, Kern K (2007) Electronic transport properties of individual chemically reduced graphene oxide sheets. *Nano Lett* 7:3499–3503
 29. Mosalman S, Rashahmadi S, Hasanzadeh R (2017) The effect of TiO₂ nanoparticles on mechanical properties of poly methyl methacrylate nanocomposites. *Int J Eng Trans B Appl* 30:807–813
 30. Alamgir M, Nayak GC, Mallick A, Tiwari SK, Mondal S, Gupta M (2018) Processing of PMMA nanocomposites containing bio-compatible GO and TiO₂ nanoparticles. *Mater Manuf Process* 33:1291–1298
 31. Hatui G, Nayak GC, Udayabhanu G (2016) One pot solvothermal synthesis of sandwich-like Mg Al layered double hydroxide anchored reduced graphene oxide: an excellent electrode material for supercapacitor. *Electrochim Acta* 219:214–226
 32. Jarrar R, Mohsin MA, Haik Y (2012) Alteration of the mechanical and thermal properties of nylon 6/nylon 6,6 blends by nanoclay. *J Appl Polym Sci* 124:1880–1890
 33. Vargün E, Usanmaz A (2010) Degradation of poly(2-hydroxyethyl methacrylate) obtained by radiation in aqueous solution. *J Macromol Sci A* 47:882–891
 34. Vasile E, Pandeale AM, Andronescu C, Selaru A, Dinescu S, Costache M, Hanganu A, Raicopol MD, Teodorescu M (2019) Hema-functionalized graphene oxide: a versatile nanofiller for poly (propylene fumarate)-based hybrid materials. *Sci Rep* 9:18685. <https://doi.org/10.1038/s41598-019-55081-2>
 35. Sabet M, Soleimani H, Mohammadian E, Hosseini S (2020) Impact of inclusion of graphene oxide nanosheets on polypropylene thermal characteristics. *Iran Polym J* 29:1099–1112
 36. Mat Yazik MH, Sultan MTH, Shah AUM, Jawaid M, Mazlan N (2020) Effect of nanoclay content on the thermal, mechanical and shape memory properties of epoxy nanocomposites. *Polym Bull* 77:5913–5931
 37. Li X, Habibnejad Korayem A, Li C, Liu Y, He H, Sanjayan JG, Duan WH (2016) Incorporation of graphene oxide and silica fume into cement paste: a study of dispersion and compressive strength. *Constr Build Mater* 123:327–335
 38. Choi Y, Lee HS, Kwon D (2004) Analysis of sharp-tip-indentation load–depth curve for contact area determination taking into account pile-up and sink-in effects. *J Mater Res* 19:3307–3315